Variational and parquet-diagram calculations for neutron matter. III. *S*-wave pairing

E. Krotscheck and J. Wang
Department of Physics, University at Buffalo, SUNY Buffalo, Buffalo, New York 14260 and
Institut für Theoretische Physik, Johannes Kepler Universität, A 4040 Linz, Austria

(Received 26 October 2020; accepted 15 February 2021; published 12 March 2021)

We apply parquet-diagram summation methods for the calculation of the superfluid gap in *S*-wave pairing in neutron matter for realistic nucleon-nucleon interactions such as the Argonne v_6 and the Reid v_6 potentials. It is shown that diagrammatic contributions that are outside the parquet class play an important role. These are, in variational theories, identified as "commutator contributions." Moreover, using a particle-hole propagator appropriate for a superfluid system results in the suppression of the spin-channel contribution to the induced interaction. Applying these corrections to the pairing interaction, our results agree quite well with quantum Monte Carlo data.

DOI: 10.1103/PhysRevC.103.035808

I. INTRODUCTION

The nature and role of fermionic pairing and superfluidity in nuclei and nuclear matter has been a subject of great interest for many years [1]. Beginning with work by Bohr, Mottelson, and Pines [2] there was persistent interest among nuclear theorists in what could be learned from the quantum many-body problem of infinite nuclear matter composed of nucleons interacting through the best nucleon-nucleon (NN) interaction available.

Bardeen-Cooper-Schrieffer (BCS) theory as originally formulated [3] is intrinsically a mean-field theory. Cooper, Mills, and Sessler [4] were the first to realize that the BCS equation *per se* could also be solved for hard-core interactions, but that still leaves the question open to what extent such a theory could capture the physics of a strongly interacting system. This issue was addressed by the introduction of Jastrow-Feenberg correlation factors [5–7]. Major advances were made with the replacement of cluster expansions by Fermi hypernetted-chain (FHNC) diagram-resummation techniques [8,9], facilitating the unconstrained optimization of Jastrow-Feenberg correlations (FHNC-Euler-Lagrange (FHNC-EL) method). The fact that optimized hypernetted-chain summations included the summations of high-order contributions to the perturbation series was first observed by Sim, Buchler, and Woo [10], it was put on a rigorous foundation in the work by Jackson, Lande, and Smith [11,12] who showed, for bosons, that the optimized hypernetted chain theory for Jastrow-Feenberg correlations is equivalent to the self-consistent summation of all ring and ladder diagrams, the "parquet" diagrams.

When implemented in a BCS extension, these advances have made possible the development of a rigorous correlated BCS (CBCS) theory (Ref. [13], see also Ref. [14]) that respects the U(1) symmetry-breaking aspect of the superfluid state—i.e.,the nonconservation of particle number. A recent in-depth study of correlations in the low-density Fermi gas [15], with emphasis on the presence of Cooper pairing and dimerization, documents the power of the Euler-Lagrange (EL) FHNC approach adopted in the present work. The major drawback of these calculations was that they employed simple state-independent correlation functions. This makes the method suitable for simple interactions, but improvements must be sought for realistic nuclear Hamiltonians.

In recent work [16,17], we have utilized the equivalence between parquet-diagram summations and optimized variational methods to develop methods that address exactly this problem. We will review these in the next section.

II. VARIATIONAL AND PARQUET-DIAGRAM THEORY

A. The normal ground state

Let us briefly describe the Jastrow-Feenberg variational and parquet-diagram summation method and its implementation to superfluid systems.

We assume a nonrelativistic many-body Hamiltonian,

$$H = -\sum_i \frac{\hbar^2}{2m}\nabla_i^2 + \sum_{i<j} v(i,j). \tag{2.1}$$

Popular models of the nucleon-nucleon force [18–22] represent the interaction as a sum of local functions times correlation operators, i.e.,

$$\hat{v}(i,j) = \sum_{\alpha=1}^{n} v_\alpha(r_{ij})\,\hat{O}_\alpha(i,j), \tag{2.2}$$

where $r_{ij} = |\mathbf{r}_i - \mathbf{r}_j|$ is the distance between particles i and j, and the $O_\alpha(i,j)$ are operators acting on the spin, isospin, and possibly the relative angular momentum variables of the individual particles. According to the number of operators n, the potential model is referred to as a v_n model potential.

Reasonably realistic models for nuclear matter keep at least the six base operators, these are

$$\begin{aligned}
\hat{O}_1(i,j;\hat{\mathbf{r}}_{ij}) &\equiv \hat{O}_c = \mathbb{1},\\
\hat{O}_3(i,j;\hat{\mathbf{r}}_{ij}) &\equiv \boldsymbol{\sigma}_i\cdot\boldsymbol{\sigma}_j,\\
\hat{O}_5(i,j;\hat{\mathbf{r}}_{ij}) &\equiv S_{ij}(\hat{\mathbf{r}}_{ij}) \equiv 3(\boldsymbol{\sigma}_i\cdot\hat{\mathbf{r}}_{ij})(\boldsymbol{\sigma}_j\cdot\hat{\mathbf{r}}_{ij}) - \boldsymbol{\sigma}_i\cdot\boldsymbol{\sigma}_j,\\
\hat{O}_{2n}(i,j;\hat{\mathbf{r}}_{ij}) &= \hat{O}_{2n-1}(i,j;\hat{\mathbf{r}}_{ij})\boldsymbol{\tau}_1\cdot\boldsymbol{\tau}_2,
\end{aligned} \tag{2.3}$$

where $\hat{\mathbf{r}}_{ij} = \mathbf{r}_{ij}/r_{ij}$. We will omit the arguments when unambiguous.

There are basically two methods of comparable diagrammatic richness for manifestly microscopic calculations of properties of such strongly interacting systems. These are the Jastrow-Feenberg variational method [23] and the parquet-diagram summations [11,12]. For Bose systems, and for purely central interactions, these two methods have been shown to lead to exactly the same equations. For a strongly interacting and translationally invariant *normal* system, the Jastrow-Feenberg method starts with an *ansatz* for the wave function, [23]

$$\Psi_0(\mathbf{r}_1,\ldots,\mathbf{r}_N) = F(\mathbf{r}_1,\ldots,\mathbf{r}_N)\Phi_0(1,\ldots,N), \tag{2.4}$$

$$F(\mathbf{r}_1,\ldots,\mathbf{r}_N) = \prod_{\substack{i,j=1\\ i<j}}^{N} f(r_{ij}), \tag{2.5}$$

where $\Phi_0(\mathbf{r}_1,\ldots,\mathbf{r}_N)$ denotes a model state, which for normal Fermi systems is a Slater determinant, and F is the correlation operator which can, of course, also contain three-body correlations. For Bose systems, $\Phi_0(1,\ldots,N) = 1$. The correlation functions $f(r_{ij})$ are obtained by minimizing the energy, i.e., by solving the Euler-Lagrange equations

$$E_0 = \frac{\langle\Psi_0|H|\Psi_0\rangle}{\langle\Psi_0\mid\Psi_0\rangle} \equiv H_{\mathbf{o}}, \tag{2.6}$$

$$\frac{\delta E_0}{\delta f}(r_{12}) = 0. \tag{2.7}$$

Evaluation of the energy (2.6) for the variational wave function [(2.4) and (2.5)] and analysis of the variational problem are carried out by cluster expansion and resummation methods. The procedure has been described at length in review articles [8,24] and pedagogical material [9].

No derivation comparable in rigor to that of Refs. [11,12] exists for fermions. We have analyzed in Ref. [25] the relationship between specific classes of diagrams generated by the cluster expansion and optimization procedure of Jastrow-Feenberg theory and classes of parquet diagrams, specifically rings, ladders, and self-energy corrections. Besides the localization procedures used to establish the agreement between the boson versions of Jastrow-Feenberg and parquet diagrams, a "collective" approximation must be made for the particle-hole propagator. Moreover, since the Fermi sea breaks Galilean invariance, specific Fermi sea averages must be made to make all two-body vertices functions of the momentum transfer only. These procedures have been discussed and examined in detail in Ref. [25].

The situation is much more complicated for realistic nuclear Hamiltoninans of the form (2.2). A plausible generalization of the Jastrow-Feenberg function (2.5) would be [26–28] the "symmetrized operator product form

$$\Psi_0^{\mathrm{SOP}} = \mathcal{S}\left[\prod_{\substack{i,j=1\\ i<j}}^{N} \hat{f}(i,j)\right]\Phi_0, \tag{2.8}$$

where

$$\hat{f}(i,j) = \sum_{\alpha=1}^{n} f_\alpha(r_{ij})\,\hat{O}_\alpha(i,j), \tag{2.9}$$

and $\mathcal{S}$ stands for symmetrization. The symmetrization is necessary because the operators $\hat{O}_\alpha(i,j)$ and $\hat{O}_\beta(i,k)$ do not necessarily commute. The need to symmetrize the operator product causes, however, severe complications and so far no summation that comes anywhere close to the diagrammatic richness of the (F)HNC summations for state-independent correlations has been found. As a consequence, no unconstrained optimization method analogous to Eq. (2.7) could be developed. Instead, the correlation functions $f_\alpha(r)$ have been either assumed to be of some simple parameterized form, or calculated by a low-order effective Schrödinger equation [low-order constrained variation (LOCV)]. Operator contributions were calculated in a chain approximation "single-operator chains" which can be understood [29] as a simplified version of the random-phase approximation. We have shown in previous work [30] that this leads to sensible results only if the commutator terms generated by the symmetrization of the correlation operator (2.9) are omitted.

In view of these complications, Smith and Jackson [31] developed the parquet-diagram summations for a fictitious system of bosons interacting via a v_6 model Hamiltonian. It turned out that the equations derived were the same as the Bose version of the hypernetted chain equations derived from a variational wave function [(2.8) and (2.9)] when all commutators are omitted, and supplemented by the optimization condition (2.7). This leads to the conclusion that the commutator diagrams correspond to diagrams in perturbation theory that are beyond the parquet class.

The physical mechanism described by commutator diagrams is exemplified in the two simple processes shown diagrammatically in Fig. 1. In the left diagram, a pair of particles that enter the process in a specific (singlet or triplet) state will always remain in that state. The red wavy lines therefore describe interactions in the *same* channel. This is not changed by the exchange of a (spin-)density fluctuation depicted by the chain of two blue lines. In the right diagram, a spin is absorbed, transported through a spin-fluctuation, described again by the chain of two blue wavy lines, and reabsorbed at a later time. In that situation, the magenta wavy line may be a triplet interaction, whereas the red lines are singlet interactions or vice versa. Evidently, this makes little difference if the interactions are the same in spin-singlet and spin-triplet states. On the other hand, there is no reason that the two processes are similar if the interactions are very different, which is the case for modern nucleon-nucleon interactions [18,21].

Taking this into account and the evidence that simplistic choices of the pair correlation functions $f_\alpha(r_{ij})$ lead to sen-

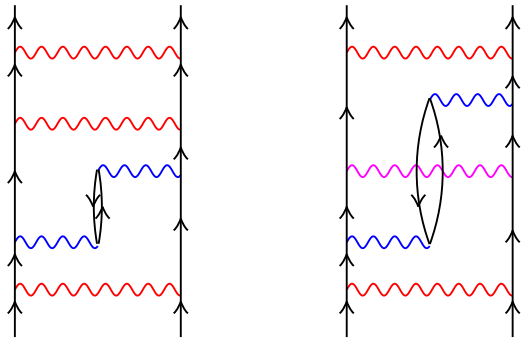

FIG. 1. The figure shows the essential processes are included in the "twisted chain" interaction correction. The red wavy lines are either spin-singlet or spin-triplet interactions, the magenta line may be either of the two, and the chain of blue lines represents a contribution to the induced interaction $\widehat{W}_I$ (from Ref. [17]).

sible results only when commutator diagrams are omitted, we have in recent work [17] added the leading corrections that capture the essential physics of the commutator diagrams. To make the method practical, we have used approximations suggested by the Jastrow-Feenberg theory and the insight about diagram topology from parquet diagram summations. The results showed that the "beyond-parquet" diagrams are, especially in low-density neutron matter and in the singlet interaction channel, more important than any other many-body corrections.

B. Strongly interacting superfluids

Let us now turn to the generalization of the correlated wave functions method to superfluid systems. Having reviewed the FHNC-EL theory and its relation to parquet diagrams above, we can restrict ourselves to the discussion of what changes for a superfluid system. Older work has either assumed that the superfluid state deviates little from the normal state [13–15,32–34] and/or adopted low-order cluster expansions [6,35–37]. In recent work [25], we have developed the Jastrow-Feenberg variational approach for a superfluid system to a level comparable to that of the normal system. This has made the identification with parquet-diagrams possible. A number of important results will be discussed below.

The basic idea of a correlated BCS state is to use for the model state in Eq. (2.4) an uncorrelated BCS state

$$|\mathrm{BCS}\rangle = \prod_{\mathbf{k}} [u_{\mathbf{k}} + v_{\mathbf{k}} a^{\dagger}_{\mathbf{k}\uparrow} a^{\dagger}_{-\mathbf{k}\downarrow}]|\,\rangle, \tag{2.10}$$

where $|\,\rangle$ is the vacuum state and the $u_{\mathbf{k}}$, $v_{\mathbf{k}}$ are the Bogoliubov amplitudes satisfying $u^2_{\mathbf{k}} + v^2_{\mathbf{k}} = 1$. A *correlated* state is then constructed by applying a correlation operator F to that state. Since the state (2.10) does not have a fixed particle number, we must write the correlated state in the form

$$|\mathrm{CBCS}\rangle = \sum_{\mathbf{m},N} |\Psi^{(N)}_{\mathbf{m}}\rangle\langle \mathbf{m}^{(N)}|\mathrm{BCS}\rangle, \tag{2.11}$$

where the $\{|\mathbf{m}^{(N)}\rangle\}$ form a complete set of N-body Slater determinants, and the $|\Psi^{(N)}_{\mathbf{m}}\rangle$ are correlated and normalized N-body states forming a nonorthogonal basis of the Hilbert space, see Eq. (A1).

In what follows, we will refer to expectation values with respect to the *uncorrelated* state (2.10) as $\langle\ldots\rangle_0$ and those with respect to the *correlated state* (2.11) as $\langle\ldots\rangle_c$. Physically interesting quantities like the (zero temperature) Landau potential of the superfluid system

$$\langle H'\rangle_c = \frac{\langle \mathrm{CBCS}|\hat{H}'|\mathrm{CBCS}\rangle}{\langle \mathrm{CBCS}|\mathrm{CBCS}\rangle}, \quad \hat{H}' \equiv \hat{H} - \mu\hat{N}, \tag{2.12}$$

are then calculated by cluster expansion and resummation techniques. Above, μ is the chemical potential.

There are basically two ways to deal with the correlated wave function (2.11).

1. Weakly coupled systems

We rely in this section heavily on definitions and methods of correlated basis functions (CBF) theory that have been discussed elsewhere [8,9,24]. To settle the notation, we give the definitions of the essential quantities in Appendix.

If the superfluid gap is small compared to the Fermi energy, then it is legitimate to simplify the problem by expanding $\langle H'\rangle_c$, Eq. (2.12) in the *deviation* of the Bogoliubov amplitudes $u_{\mathbf{k}}$, $v_{\mathbf{k}}$ from their normal state values $u^{(0)}_{\mathbf{k}} = \bar{n}(k)$, $v^{(0)}_{\mathbf{k}} = n(k)$, where $n(k) = \theta(k_F - k)$ is the Fermi distribution and $\bar{n}(k) = 1 - n(k)$. This approach adopts a rather different concept than the original BCS theory: A wave function of the form (2.10) begins by creating Cooper pairs out of the vacuum. Instead, the approach (2.11) begins with the *normal, correlated* ground state and generates one Cooper pair at a time out of the normal system as suggested recently by Leggett [38]. Adopting such an expansion in the number of Cooper pairs, the correlation functions $f(r_{ij})$ and possibly higher-order correlations can be optimized for the normal system.

Carrying out this expansion in the number of Cooper pairs, we have arrived in Ref. [13] at the energy expression of the superfluid state

$$\begin{aligned}\langle \hat{H}'\rangle_c \;=\; & E_0 - \mu N + 2\sum_{\mathbf{k},\,|\,\mathbf{k}\,|\,>k_F} v^2_{\mathbf{k}}(e_{\mathbf{k}} - \mu) - 2 \\ & \times \sum_{\mathbf{k},\,|\,\mathbf{k}\,|\,<k_F} u^2_{\mathbf{k}}(e_{\mathbf{k}} - \mu) \\ & + \sum_{\mathbf{k},\mathbf{k}'} u_{\mathbf{k}} v_{\mathbf{k}} u_{\mathbf{k}'} v_{\mathbf{k}'} \mathcal{P}_{\mathbf{k}\mathbf{k}'}. \end{aligned} \tag{2.13}$$

Above, $E_0 \equiv H^{(N)}_{\mathbf{o}}$ is the energy expectation value (2.6) of the normal N-particle system. The $e_{\mathbf{k}}$ are the single-particle energies derived in CBF theory [39], see Appendix. The paring interaction has the form

$$\mathcal{P}_{\mathbf{k}\mathbf{k}'} = \mathcal{W}_{\mathbf{k}\mathbf{k}'} + (|e_{\mathbf{k}} - \mu| + |e_{\mathbf{k}'} - \mu|)\mathcal{N}_{\mathbf{k}\mathbf{k}'}, \tag{2.14}$$

$$\mathcal{W}_{\mathbf{k}\mathbf{k}'} = \langle \mathbf{k}\uparrow, -\mathbf{k}\downarrow|\mathcal{W}(1,2)|\mathbf{k}'\uparrow, -\mathbf{k}'\downarrow\rangle_a, \tag{2.15}$$

$$\mathcal{N}_{\mathbf{k}\mathbf{k}'} = \langle \mathbf{k}\uparrow, -\mathbf{k}\downarrow|\mathcal{N}(1,2)|\mathbf{k}'\uparrow, -\mathbf{k}'\downarrow\rangle_a. \tag{2.16}$$

The effective interaction $\mathcal{W}(1,2)$ and the correlation corrections $\mathcal{N}(1,2)$ are given by the compound-diagrammatic

ingredients of the FHNC-EL method for off-diagonal quantities in CBF theory [39].

The Bogoliubov amplitudes $u_{\mathbf{k}}$, $v_{\mathbf{k}}$ are obtained in the standard way by variation of the energy expectation (2.13). This leads to the familiar gap equation

$$\Delta_{\mathbf{k}} = -\frac{1}{2}\sum_{\mathbf{k}'} \mathcal{P}_{\mathbf{k}\mathbf{k}'} \frac{\Delta_{\mathbf{k}'}}{\sqrt{(e_{\mathbf{k}'}-\mu)^2+\Delta_{\mathbf{k}'}^2}}. \tag{2.17}$$

The conventional (i.e., "uncorrelated" or "mean-field") BCS gap equation [40] is retrieved by replacing the effective interaction $\mathcal{P}_{\mathbf{k}\mathbf{k}'}$ matrix elements by the matrix elements of the bare interaction.

2. *Strongly coupled superfluids*

The above treatment of a superfluid state has a number of appealing features. One is that the theory can me mapped onto an ordinary BCS theory, where the effective interactions and, if applicable, the single-particle spectrum, are calculated for the normal system. The other is that no assumptions need to be made on the correlation operator other than that the relevant matrix elements can be calculated with sufficient accuracy.

The basic assumption of the "weak-coupling" approximation is that the superfluid gap at the Fermi surface is small compared to the Fermi energy. This assumption is not met in low-density neutron matter where the gap energy can indeed be of the order of half of the Fermi energy; this is a common feature of practically all neutron matter gap calculations since the 1970s [6] until recently [32,41]. To examine this problem, we have derived in Ref. [25] the full variational and Fermi-HNC theory for a superfluid state of the form (2.11). Without going into the gory details of this derivation, we mention for the expert only the central feature: The exchange line

$$\ell(rk_F) = \frac{\nu}{N}\sum_{\mathbf{k}} n(k) e^{i\mathbf{k}\cdot\mathbf{r}} \tag{2.18}$$

is replaced by two types of lines,

$$\ell_v(r) \equiv \frac{\nu}{N}\sum_{\mathbf{k}} v_{\mathbf{k}}^2 e^{i\mathbf{k}\cdot\mathbf{r}} \quad \text{and} \quad \ell_u(r) \equiv \frac{\nu}{N}\sum_{\mathbf{k}} u_{\mathbf{k}} v_{\mathbf{k}} e^{i\mathbf{k}\cdot\mathbf{r}}, \tag{2.19}$$

where $\nu = 2$ is the degree of degeneracy of the single-particle states and $N = \nu\sum_{\mathbf{k}} v_{\mathbf{k}}^2$. The resulting gap equation is the same as Eq. (2.17), the only difference being that the ingredients $\mathcal{W}(1,2)$ and $\mathcal{N}(1,2)$ should be determined self-consistently for a superfluid system and depend implicitly on the $\ell_v(r)$ and $\ell_u(r)$.

The second result is more subtle and deserves further discussion: The Euler equation (2.7) for a superfluid correlated state leads to physically incorrect solutions, in fact it has no solutions for systems that are attractive in the sense that the Landau parameter $F_0^s < 0$.

C. Analysis of effective interactions

The understanding of the above-mentioned unphysical solutions of the Euler equations, the construction of effective interactions, and their choice and consequences for the pairing problem are closely related. To explain the situation, we must briefly review the relationship between FHNC-EL theory and parquet diagram summations. We do this for the simplest case that higher-order exchange diagrams are omitted; these are quantitatively important even in the low-density limit [25], but do not change the message of our analysis.

The summation of parquet diagrams implies, among others, the summation of ring diagrams with a local "particle-hole" interaction $\tilde{V}_{\mathrm{p-h}}(q)$. The long-wavelength limit is related to the Fermi liquid parameter

$$\tilde{V}_{\mathrm{p-h}}(0+) = \frac{2m}{3m^*}F_0^s. \tag{2.20}$$

One should not expect that this relationship is satisfied exactly [42] when $\tilde{V}_{\mathrm{p-h}}(0+)$ is obtained by diagram summations, and F_0^s is from hydrodynamic derivatives; the (dis-)agreement can be taken as a test for the accuracy of the implementation of the theory [16,25].

The density-density response function is in that case

$$\chi(q,\omega) = \frac{\chi_0(q,\omega)}{1-\tilde{V}_{\mathrm{p-h}}(q)\chi_0(q,\omega)}, \tag{2.21}$$

where $\chi_0(q,\omega)$ is the Lindhard function [43]. The static structure function $S(q)$ is related to the density-density response function $\chi(q,\omega)$ through

$$S(q) = -\int_0^\infty \frac{d\hbar\omega}{\pi}\mathrm{Im}\chi(q,\omega). \tag{2.22}$$

The connection to the Euler equation (2.7) of the FHNC-EL theory is established by assuming a "collective" approximation for the Lindhard function which is constructed such that the ω^0 and ω^1 sum rules are satisfied,

$$\begin{aligned} &-\mathrm{Im}\int_0^\infty \frac{d\hbar\omega}{\pi}\chi_0^{\mathrm{coll}}(q,\omega) \\ &\quad = -\mathrm{Im}\int_0^\infty \frac{d\hbar\omega}{\pi}\chi_0(q,\omega) = S_F(q), \end{aligned} \tag{2.23}$$

$$\begin{aligned} &-\mathrm{Im}\int_0^\infty \frac{d\hbar\omega}{\pi}\omega\chi_0^{\mathrm{coll}}(q,\omega) \\ &\quad = -\mathrm{Im}\int_0^\infty \frac{d\hbar\omega}{\pi}\omega\chi_0(k,\omega) = t(q), \end{aligned} \tag{2.24}$$

where $t(q) = \hbar^2q^2/2m$ and $S_F(q)$ is the static structure function of the noninteracting Fermi system. This leads to

$$\chi_0^{\mathrm{coll}}(q,\omega) = \frac{2t(q)}{(\hbar\omega+i\eta)^2 - \left[\frac{t(q)}{S_F(q)}\right]^2} \tag{2.25}$$

and, consequently, to the collective approximation for the density-density response function

$$\chi^{\mathrm{coll}}(q,\omega) = \frac{2t(q)}{(\hbar\omega+i\eta)^2 - \left[\frac{t(q)}{S_F(q)}\right]^2 - 2t(q)\tilde{V}_{\mathrm{p-h}}(q)}. \tag{2.26}$$

In this case, the frequency integration (2.22) can be carried out analytically, which leads to the simplest form of the Euler

equation of FHNC-EL theory [24],

$$S(q) = \frac{S_F(q)}{\sqrt{1 + \frac{2S_F^2(q)}{t(q)}\tilde{V}_{\rm p-h}(q)}}. \tag{2.27}$$

Since $S(q) \propto q$ for $q \to 0+$, negative values of $\tilde{V}_{\rm p-h}(q)$ and, hence, negative values of F_0^s are permitted.

In the superfluid system, the variational principle (2.7) leads to the same equation (2.27), a small additional term [25] does not change our analysis. However, the static structure function has the form

$$S_F(q) = 1 - \frac{\rho}{\nu}\int d^3r e^{i\mathbf{q}\cdot\mathbf{r}}\big[\ell_v^2(r) - \ell_u^2(r)\big]. \tag{2.28}$$

It follows immediately from the definitions (2.19) that the long-wavelength limit of $S_F(q)$ is

$$S_F(0+) = 2\frac{\sum_{\mathbf{k}} u_{\mathbf{k}}^2 v_{\mathbf{k}}^2}{\sum_{\mathbf{k}} v_{\mathbf{k}}^2} > 0. \tag{2.29}$$

Hence, $S_F(0+) > 0$ for the superfluid system. As a consequence, Eq. (2.27) has no sensible solution of $F_0^s < 0$ even for an infinitesially small but finite gap.

The problem is readily solved by abandoning the "collective" approximation (2.26), in other words moving from the pure Jastrow-Feenberg wave function to the parquet summations. There have been several suggestions for a Lindhard function for a superfluid system [44–47], the most frequently used form for $T = 0$ is given below. In the superfluid case, $\chi_0(q, \omega)$ also depends on the spins. In terms of the usual relationships of BCS theory,

$$u_k^2 = \frac{1}{2}\left(1 + \frac{\xi_{\mathbf{k}}}{E_{\mathbf{k}}}\right) \quad v_k^2 = \frac{1}{2}\left(1 - \frac{\xi_{\mathbf{k}}}{E_{\mathbf{k}}}\right), \tag{2.30}$$

with $\xi_{\mathbf{k}} = t(k) - \mu$ and $E_{\mathbf{k}} = \sqrt{\xi_{\mathbf{k}}^2 + \Delta_{\mathbf{k}}^2}$ we have [44,48–50]

$$\chi_0^{(\rho,\sigma)}(\mathbf{k}, \omega) = \frac{\nu}{N}\sum_{\mathbf{p}} b_{\mathbf{p},\mathbf{k}}^{(\rho,\sigma)}\left[\frac{1}{\hbar\omega - E_{\mathbf{k}+\mathbf{p}} - E_{\mathbf{p}} + i\eta} - \frac{1}{\hbar\omega + E_{\mathbf{k}+\mathbf{p}} + E_{\mathbf{p}} + i\eta}\right] \tag{2.31}$$

with

$$b_{\mathbf{p},\mathbf{k}}^{(\rho,\sigma)} = \frac{1}{4}\left[\left(1 - \frac{\xi_{\mathbf{p}}}{E_{\mathbf{p}}}\right)\left(1 + \frac{\xi_{\mathbf{k}+\mathbf{p}}}{E_{\mathbf{k}+\mathbf{p}}}\right) \pm \frac{\Delta_{\mathbf{p}}}{E_{\mathbf{p}}}\frac{\Delta_{\mathbf{k}+\mathbf{p}}}{E_{\mathbf{k}+\mathbf{p}}}\right] = v_{\mathbf{p}}^2 u_{\mathbf{k}+\mathbf{p}}^2 \pm u_{\mathbf{p}} v_{\mathbf{p}} u_{\mathbf{k}+\mathbf{p}} v_{\mathbf{k}+\mathbf{p}}, \tag{2.32}$$

where the upper sign applies to the density channel and the lower to the spin channel, respectively.

A similar analysis applies to the effective interaction $\mathcal{W}(1, 2)$ and the energy numerator term $\mathcal{N}(1, 2)$. In principle, these two quantities are nonlocal two-body operators. The leading, local contributions to these operators are readily expressed in terms of the diagrammatic quantities of FHNC-EL theory [24]:

$$\mathcal{N}(1, 2) = \mathcal{N}(r_{12}) = \Gamma_{\rm dd}(r_{12}), \quad \mathcal{W}(1, 2) = W(r_{12}), \tag{2.33}$$

where $\Gamma_{\rm dd}(r_{12})$ is the "direct correlation function" of FHNC theory [8,24]. In an approximation corresponding to the one spelled out in Eqs. (2.27) we have

$$\tilde{\Gamma}_{\rm dd}(q) = \frac{1}{S_F(q)}\left\{\left[1 + \frac{2S_F^2(q)}{t(q)}\tilde{V}_{\rm p-h}(q)\right]^{-1/2} - 1\right\}, \tag{2.34}$$

$$\widetilde{W}(q) = \frac{t(q)}{S_F^2(q)}\left\{1 - \left[1 + \frac{2S_F^2(q)}{t(q)}\tilde{V}_{\rm p-h}(q)\right]^{-1/2}\right\} = -\frac{t(q)}{S_F(q)}\tilde{\Gamma}_{\rm dd}(q). \tag{2.35}$$

These relationships display the same problems as the $S(q)$ above, namely that they lead to unphysical results for negative F_0^s. The solution is again found by examining the construction of $\widetilde{W}(q)$ from the viewpoint of perturbation theory.

Equation (2.21) defines an *energy-dependent* effective interaction $\widetilde{W}(q, \omega)$ which we write as the sum of the energy-independent term $\tilde{V}_{\rm p-h}(q)$ and the energy-dependent induced interaction $\widetilde{W}_I(q, \omega)$

$$\widetilde{W}(q, \omega) = \frac{\tilde{V}_{\rm p-h}(q)}{1 - \tilde{V}_{\rm p-h}(q)\chi_0(q, \omega)} = \tilde{V}_{\rm p-h}(q) + \frac{\tilde{V}_{\rm p-h}^2(q)\chi_0(q, \omega)}{1 - \tilde{V}_{\rm p-h}(q)\chi_0(q, \omega)}. \tag{2.36}$$

An *energy-independent* effective interaction $\widetilde{W}(q)$ is then defined such that it leads to the same $S(q)$, i.e.,

$$\begin{aligned} S(q) &= -\int_0^\infty \frac{d\hbar\omega}{\pi}\mathrm{Im}\frac{\chi_0(q, \omega)}{1 - \tilde{V}_{\rm p-h}(q)\chi_0(q, \omega)} \\ &= -\int_0^\infty \frac{d\hbar\omega}{\pi}\mathrm{Im}\big[\chi_0(q, \omega) + \chi_0^2(q, \omega)\widetilde{W}(q, \omega)\big] \\ &\overset{!}{=} -\int_0^\infty \frac{d\hbar\omega}{\pi}\mathrm{Im}\big[\chi_0(q, \omega) + \chi_0^2(q, \omega)\widetilde{W}(q)\big], \end{aligned} \tag{2.37}$$

where the last line defines $\widetilde{W}(q)$ and, through Eq. (2.36), the static induced interaction $\widetilde{W}_I(q) = \widetilde{W}(q) - \tilde{V}_{\rm p-h}(q)$. If we furthermore use the collective approximation (2.26) for $\chi_0(q, \omega)$, then Eq. (2.35) follows.

Realizing these connections there is, of course, no reason for not using the full Lindhard functions for defining the effective interaction $\widetilde{W}(q)$ in (2.37). This can be done using the Lindhard function for the normal system, or (2.31). The latter is numerically rather demanding, we have carried this out in Ref. [25]. It turns out that the use of (2.31) makes little difference for $\tilde{V}_{\rm p-h}(q)$, we have therefore used in our ground-state calculations the Lindhard function for the normal system.

This is different for the gap equation, partly due to the exponential dependence of the superfluid gap on the interaction strength. We have therefore used (2.31) and $\omega = 0$ for the effective interactions in the pairing calculation which is more appropriate for these low-energy phenomena [51].

D. Analysis of the gap equation

The appearance of the "energy numerator" term in the pairing interaction matrix element (2.14) is a feature that might be unfamiliar to the reader who is only familiar with mean-field theories, but it comes in quite naturally when the gap equation is expressed in terms of the T matrix [52]. This section is devoted to a discussion of the importance of this term which arises in an expansion of the correlated BCS state (2.11) in the number of Cooper pairs. We stress again that no assumption on the nature of the correlation operator has been made in the derivation.

If the gap at the Fermi surface is small, then we can replace the pairing interaction $\tilde{\mathcal{W}}(k)$ by its S-wave matrix element at the Fermi surface,

$$\tilde{\mathcal{W}}_F \equiv \frac{1}{2k_F^2}\int_0^{2k_F} kdk\widetilde{W}(k) = N\mathcal{W}_{k_F,k_F}. \tag{2.38}$$

Then we can write the gap equation as

$$1 = -\tilde{\mathcal{W}}_F \int \frac{d^3k'}{(2\pi)^3\rho}\left[\frac{1}{\sqrt{(e_{k'}-\mu)^2+\Delta_{k_F}^2}} - \frac{|e_{k'}-\mu|}{\sqrt{(e_{k'}-\mu)^2+\Delta_{k_F}^2}}\frac{S_F(k')}{t(k')}\right], \tag{2.39}$$

which is almost identical to Eq. (16.91) in Ref. [52]. In particular, the second term, which originates from the energy numerator generated in Eq. (2.17) by the second term of $\mathcal{P}_{\mathbf{kk}'}$ in Eq. (2.14), has the function of regularizing the integral for large k'.

This observation leads us to two conclusions: First, the effective interaction $\widetilde{W}(k)$ should be identified with a local approximation to the T-matrix. This is also evident because its diagrammatic structure contains both particle-particle and particle-hole reducible diagrams. Second, a correct balance between the energy numerator and the interaction term are essential to guarantee the convergence of the integral.

When the gap is large, one can no longer argue that the energy numerator, which vanishes at the Fermi surface, is negligible. The convergence of the integrals is, in this case, guaranteed by the fact that the interactions fall off for large k'. Since the integrals would diverge if the interactions did not fall off, the precise asymptotic form can have a profound quantitative influence on the magnitude of the gap.

To be more precise, we can again study the behavior of the integrand for large k':

$$\begin{aligned}\mathcal{P}_{\mathbf{kk}'} &= \mathcal{W}_{\mathbf{kk}'} + (|e_{\mathbf{k}}-\mu| + |e_{\mathbf{k}'}-\mu|)\mathcal{N}_{\mathbf{kk}'} \\ &\to \mathcal{W}_{0,\mathbf{k}'} + t(k')\mathcal{N}_{0,\mathbf{k}'}.\end{aligned} \tag{2.40}$$

From Eq. (2.35) we can now conclude that these two terms always cancel for large arguments.

The cancellation of these two terms is, of course, a consequence of either the functional optimization of the correlations or the parquet diagram summations. It is therefore expected that the actual value of the gap depends sensitively on how the energy numerator is treated. This also applies to the question of how one should deal with a nontrivial single-particle spectrum; comments on this are found in Ref. [32]. Similar concerns apply to calculations that use state-independent correlation functions of the form (2.5), including our own work [32]: The correlations are optimized for the central channel of the interaction, but the paring interaction is calculated in the singlet-S channel. Hence, the cancellations between energy numerator and interaction term are violated. The alternative, namely calculating the correlations for a model where the singlet-S channel is taking as state-independent interaction, is not a viable one because such a system would become unstable against infinitesimal density fluctuations at densities much smaller than those of interest here.

Finally, we go back to the seminal paper by Cooper, Mills, and Sessler [4], who showed that the gap equation has indeed solutions for interactions with strongly repulsive cores. Taming the strongly repulsive core of the nucleon-nucleon interaction was also the original intention of the Jastrow method [53], one might therefore legitimately ask if using Jastrow correlation in combination with a BCS state does not double count the short-ranged correlations.

As long as the theory is based on a clean expansion in the number of Cooper pairs, there is by construction no overcounting problem, but it is instructional to see the interplay between Jastrow-correlations and BCS correlations. To see that, it is sufficient to examine the two-body approximation which is still occasionally being used [35–37,54]. We also restrict ourselves, for simplicity, to state-independent correlations. In that approximation, we have

$$\begin{aligned}W^{(2)}(r) &= f^2(r)v(r) + \frac{\hbar^2}{m}|\nabla f(r)|^2, \\ \Gamma_{\mathrm{dd}}^{(2)}(r) &= f^2(r) - 1 \equiv h(r).\end{aligned} \tag{2.41}$$

Following Ref. [4], Eq. (15), we introduce

$$\tilde{\chi}(k) = \frac{1}{2}\frac{\Delta_{\mathbf{k}'}}{\sqrt{(e_{\mathbf{k}'}-\mu)^2+\Delta_{\mathbf{k}'}^2}}. \tag{2.42}$$

The short-ranged structure of the correlations is determined by the short-wavelength behavior of the gap equation, in that case we get for the coordinate space representation of the right-hand side of the gap equation as

$$\begin{aligned}&\left[-\frac{\hbar^2}{2m}\nabla^2-\mu\right]h(r)\chi(r) + h(r)\left[-\frac{\hbar^2}{2m}\nabla^2-\mu\right]\chi(r) + \left[f^2(r)v(r)+\frac{\hbar^2}{m}|\nabla f(r)|^2\right]\chi(r) \\ &\quad = f(r)\chi(r)\left[-\frac{\hbar^2}{m}\nabla^2+v(r)\right]f(r) - \frac{\hbar^2}{m}\nabla\cdot(h(r)\nabla\chi(r)) - 2\mu h(r)\chi(r).\end{aligned} \tag{2.43}$$

Above, the first two terms come from the energy numerator and the last from the interaction. If we assume that the correlation function is determined by a Schrödinger-like equation as, for example, in the LOCV method, then the Jastrow correlation function serves to cancel the short-ranged interaction. Combining these terms as in the second line shows how the Jastrow correlation function $f(r)$ eliminates the short-ranged part of the interaction, leaving $\chi(r)$ to deal with BCS-specific correlations. On the other hand, ignoring the energy numerator term destroys this cancellation.

A further evidence for the delicate balance between the two terms in the pairing interaction (2.14) is uncovered by calculating the particle-hole average

$$\sum_{\rm ph}[\mathcal{W}_{\mathbf{ph}'} + (|e_{\mathbf{p}} - \mu| + |e_{\mathbf{h}} - \mu|)\mathcal{N}_{\mathbf{ph}}] = \sum_{\rm ph}[\mathcal{W}_{\mathbf{ph}} + (e_{\mathbf{p}} - e_{\mathbf{h}})\mathcal{N}_{\mathbf{ph}}].$$

Using a free single-particle spectrum and the local approximations (2.34) and (2.35), we find that this average is zero. This is actually only a special case of a more general statement that the particle-hole average of CBF effective interaction is zero for optimized correlation functions.

This means, of course, that both the "average zero" property and the cancellation of the short-ranged structure of the interaction does not apply for cases where the correlation functions are optimized for, say, the central part of the interaction, but then the singlet projection is used for the pairing calculation.

III. APPLICATION TO NEUTRON MATTER

A. General remarks

We have carried out calculations for static properties and superfluid pairing gaps in neutron matter based on two representative NN interactions acting in the $T = 1$ channel, namely the v_6 version of the Reid soft-core potential [18] as formulated in Eqs. (A1)–(A8) of Ref. [20], and the Argonne v_6 potential [21]. Several types of calculations were done: Parquet calculations as described in Ref. [16], and parquet calculations including the most important nonparquet corrections, the "twisted chain" diagrams [17]. The calculations for the ground-state calculations were all done for the normal system. We have, in Ref. [25], also used the superfluid Lindhard functions (2.31) which requires a rather demanding numerical calculation to capture the sharp structures of the integrands around the Fermi surface. In that work, we have determined that this causes no visible change in the essential inputs for the pairing interaction, even if the gap is of the order of half the Fermi energy.

For the calculation of the effective interactions, we have used both the normal Lindhard function as well as the generalizations (2.31) to superfluid systems.

B. Effective interactions

Let us return to the effective interactions (2.35). Following the discussions of Secs. II C and II D, we can write the induced interaction in the state-dependent parquet scheme as

$$\widetilde{W}_I^{(\alpha)}(q,0) = \frac{\left[\tilde{V}_{\rm p-h}^{(\alpha)}(q)\right]^2 \chi_0^{(\alpha)}(q,0)}{1 - \tilde{V}_{\rm p-h}^{(\alpha)}(q)\chi_0^{(\alpha)}(q,0)}. \tag{3.1}$$

where the superscript α refers to the operator channel $\mathbb{1}$, $\hat{L} \equiv (\boldsymbol{\sigma}_1 \cdot \hat{\mathbf{r}})(\boldsymbol{\sigma}_2 \cdot \hat{\mathbf{r}})$, and $\hat{T} \equiv \boldsymbol{\sigma}_1 \cdot \boldsymbol{\sigma}_2 - (\boldsymbol{\sigma}_1 \cdot \hat{\mathbf{r}})(\boldsymbol{\sigma}_2 \cdot \hat{\mathbf{r}})$.

We have included in the induced interaction $\widetilde{W}_I(q) \equiv \widetilde{W}_I(q, \omega = 0)$ the leading exchange diagram which are important to establish a reasonable agreement between the long-wavelength limit of the particle-hole interaction and Landau's Fermi-liquid parameter F_0^s, i.e.,we use for the particle-hole interaction in Eq. (2.36) in the $\{\mathbb{1}, \hat{L}, \hat{T}\}$ channel basis

$$\tilde{V}_{\rm p-h}^{(\alpha)}(q) = \tilde{V}_{\rm p-h,d}^{(\alpha)}(q) + \tilde{V}_{\rm p-h,ex}^{(\alpha)}(q), \tag{3.2}$$

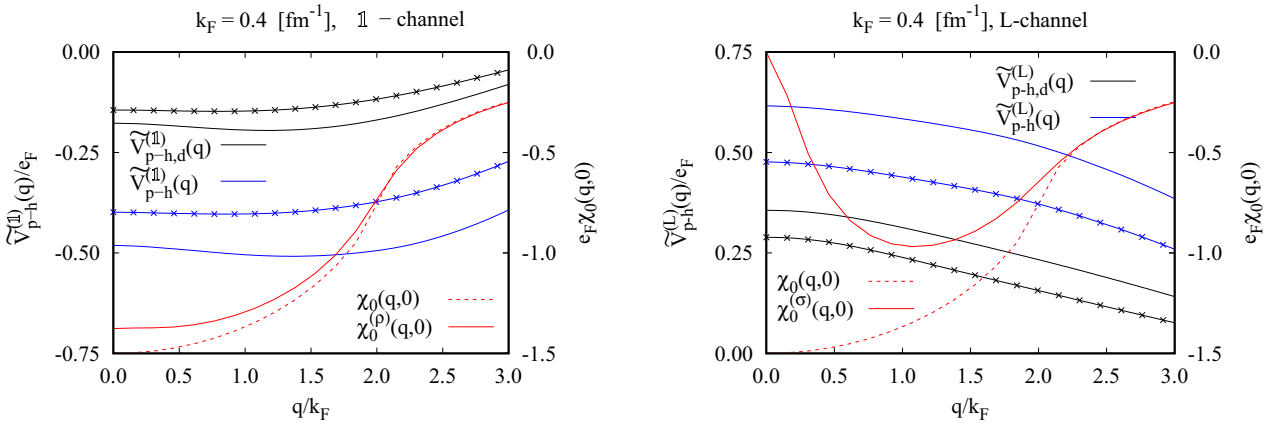

FIG. 2. The figures show, for $k_F = 0.4$ fm^{-1}, the central and longitudinal components of both the "direct" particle-hole interaction $\tilde{V}_{\rm p-h,d}^{(\alpha)}(q)$ (black lines, left scale), and effective interaction including exchange diagrams $\tilde{V}_{\rm p-h}^{(\alpha)}(q) \equiv \tilde{V}_{\rm p-h,d}^{(\alpha)}(q) + \tilde{V}_{\rm p-h,ex}^{(\alpha)}(q)$ (blue lines, left scale.) We show both the parquet results and those including nonparquet corrections (lines with markers). Also shown are the normal system Lindhard function (red dashed line, right scale) and the superfluid system Lindhard function (red solid line) in the density (left panel) and spin channel (right panel), respectively.

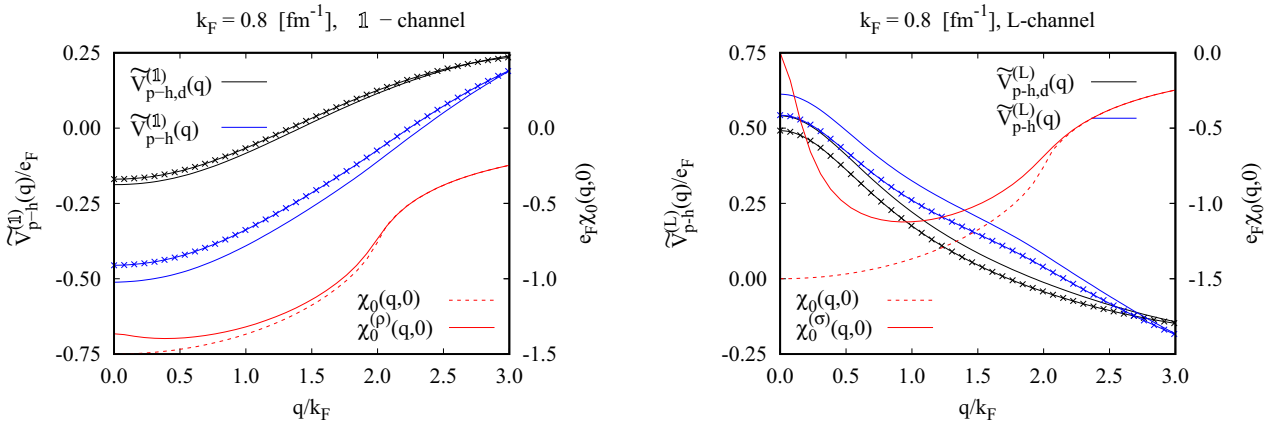

FIG. 3. Same as Fig. 2 for $k_F = 0.8$ fm^{-1}.

where the $\tilde{V}^{(\alpha)}_{\mathrm{p-h,ex}}(q)$ is calculated as spelled out in the Appendix of Ref. [16] and $\chi_0^{(L)}(q,0) = \chi_0^{(T)}(q,0) \equiv \chi_0^{(\sigma)}(q,0)$. One can go beyond this relatively simple approximation and include higher-order exchange diagrams, these would, among others, establish the correct relationships between the sum rules for the Fermi liquid parameters and those for the forward scattering amplitudes [55]. The effect may be important at higher densities and in the case of P-wave pairing [56]. However, the most important input to the calculation is the particle-hole irreducible interaction $\hat{V}_{\mathrm{p-h}}(q)$. This should *not* be identified with some local approximation of the G matrix. This is seen most easily in a self-bound system like nuclear matter by the simple argument that the Fermi-sea average of the G matrix should basically be the interaction correction to the binding energy which is negative. On the other hand, the matrix element of $V^{(\mathbb{1})}_{p-h}(r)$ at the Fermi surface is the interaction correction to the incompressibility which is positive [57]. The more important consideration is, in our opinion, to establish a reasonably accurate agreement between the long-wavelength limit (2.20) and the hydrodynamic compressibility

$$mc^2 = \frac{d}{d\rho}\rho^2\frac{d}{d\rho}\frac{E}{N} = mc_F^{*2} + \tilde{V}_{\mathrm{p-h}}(0+) \equiv mc_F^{*2}\left(1 + F_0^S\right), \tag{3.3}$$

where $c_F^* = \sqrt{\frac{\hbar^2 k_F^2}{3mm^*}}$ is the speed of sound of the noninteracting Fermi gas with the effective mass m^*. We have discussed this issue in Ref. [16].

Our work goes beyond previous calculations in two important aspects. One is the full execution of the localized parquet diagrams, including the "twisted chain" diagrams that go beyond the parquet class. The second is the use of a Lindhard function (2.31) appropriate for superfluid systems. Both of these corrections are expected to be most visible at low densities but for different reasons:

The bare singlet interaction is close to forming a bound state; therefore a small change in the effective interaction

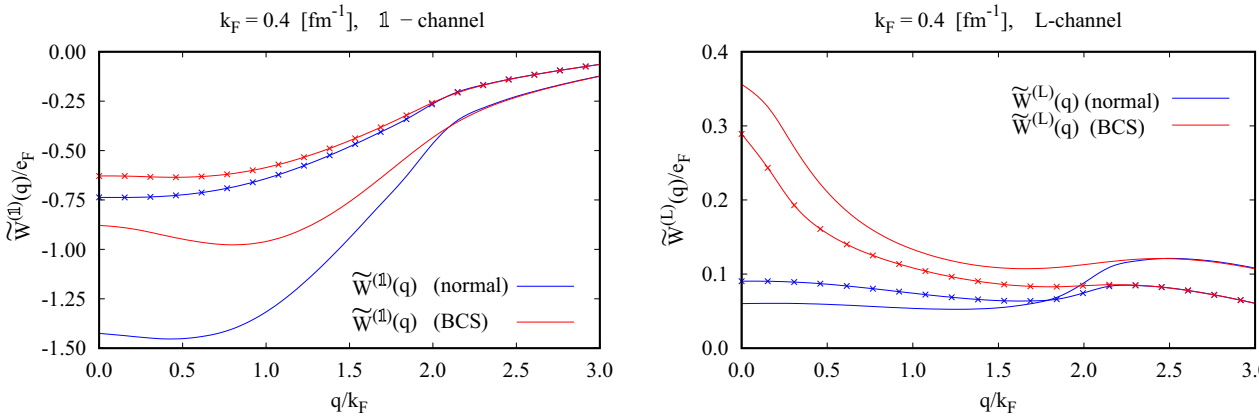

FIG. 4. The figures shows, for $k_F = 0.4$ fm^{-1}, the central (left figure) and longitudinal components (right figure) of the effective interactions $\tilde{W}^{(\alpha)}(q)$, using the normal system Lindhard functions (blue lines) and the superfluid system Lindhard functions (red lines). The results including "beyond parquet" diagrams are marked with crosses.

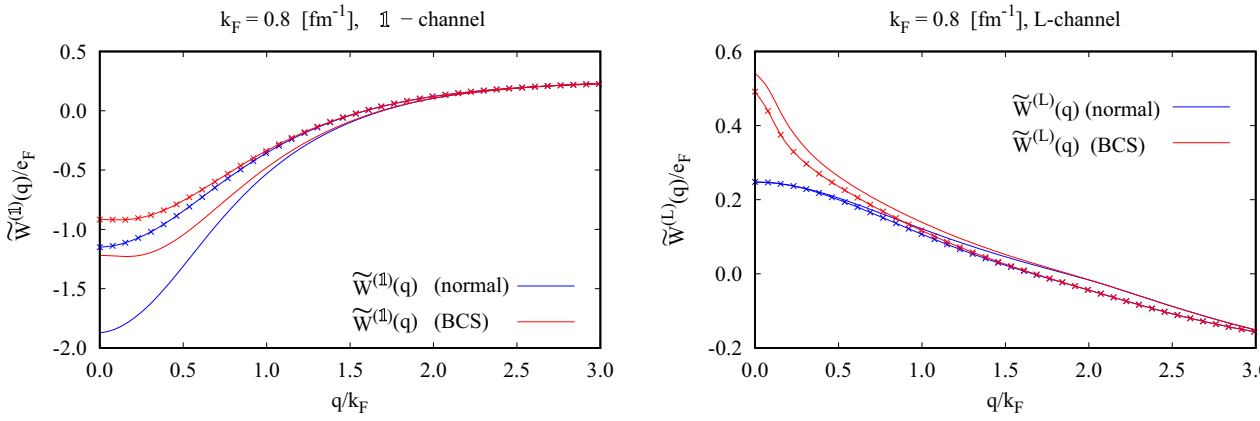

FIG. 5. Same as Fig. 4 for $k_F = 0.8$ fm^{-1}.

can cause a rather large change in the short-ranged correlations [58]. A very careful evaluation of all relevant quantities is therefore essential.

Moreover, at low densities, the superfluid gap is about half of the Fermi energy, therefore there is no reason to assume that the use of a Lindhard function appropriate for a normal system is justified. Note also that $\lim_{q\to 0}\chi^{(\sigma)}(q,0) = 0$, i.e.,the use of a superfluid Lindhard function suppresses the induced interactions $\widetilde{W}^{(L)}(q)$ and $\widetilde{W}^{(T)}(q)$ in the long-wavelength limit.

Let us therefore go through the individual steps. All calculations refer to the v_6 version of the Argonne potential [21], we have chosen a density of $k_F = 0.4$ fm^{-1} where the superfluid gap is close to its maximum value as a function of density, and to $k_F = 0.8$ fm^{-1}, where it is declining but still visible. Input to the calculations are the particle-hole irreducible interactions $\tilde{V}^{(\alpha)}_{\rm p-h}(q)$ and the Lindhard functions $\chi_0^{(\alpha)}(q,0)$. We show these for the above two typical values of k_F in Figs. 2 and 3.

Practically all of these results look rather innocuous. As shown in our previous work [16], the inclusion of exchange diagrams is important to have a reasonably accurate relationship between the Fermi liquid parameters obtained from hydrodynamic derivatives and the long-wavelength limit of the particle-hole interaction. The "twisted chain" diagrams are the most pronounced many-body correction at low densities [17], but their effect is moderate. Considering the exponential dependence of the superfluid gap on the interaction strength, these processes can, of course, be quantitatively relevant.

The superfluid Lindhard function deviates, in the density channel, by about 10 to 20 percent from the normal system Lindhard function. The most pronounced new effect is that the superfluid Lindhard function in the spin channel, $\chi_0^{(\sigma)}(q,0)$, goes to zero in the long wavelength limit. At low densities, $k_F = 0.4$ fm^{-1}, this falloff already happens at $q = k_F$ which has the effect of suppressing the induced interaction. As expected, all corrections become smaller with increasing density. In the case of the superfluid Lindhard function, this is partly the case due to the smaller value of the gap, but evidently the correction in the spin channel is still quite visible.

Turning to the interactions that actually go into the gap equation, we show in Figs. 4 and 5 the interaction $\widetilde{W}(q)$ appearing in Eq. (2.15). A somewhat surprising, but easily understood, feature is the rather dramatic consequence of using the superfluid Lindhard function in the density channel: The fact that the long-wavelength limit $\tilde{V}_{\rm p-h}(0+)$ is of the order

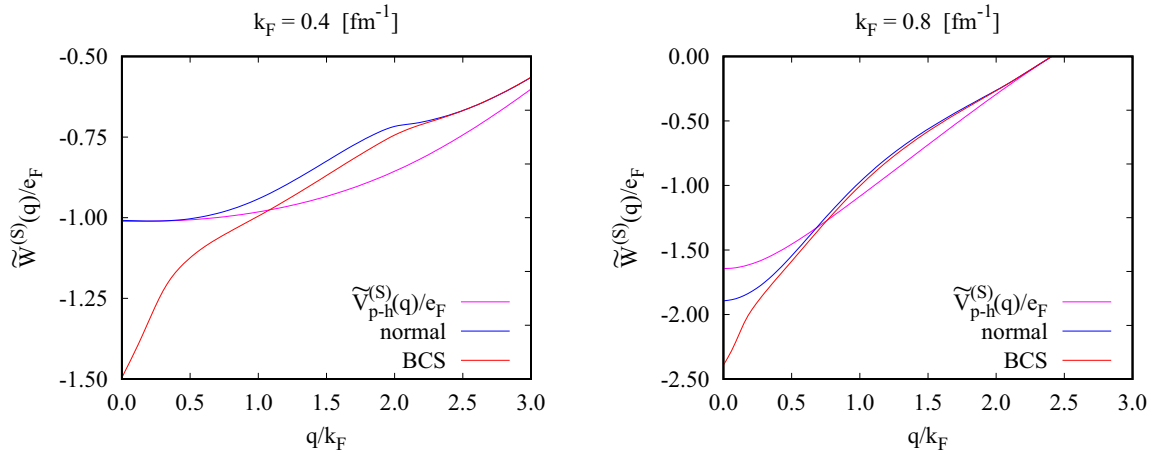

FIG. 6. The left figures shows, for $k_F = 0.4$ fm^{-1}, the singlet-S-wave effective interaction, using both the normal system Lindhard function (blue line) and the superfluid Lindhard function (red line). Also shown is the "direct" part of the particle-hole interaction (magenta line). The right figure shows the same potentials at $k_F = 0.8$ fm^{-1}. Both figures refer to the "beyond parquet" calculation.

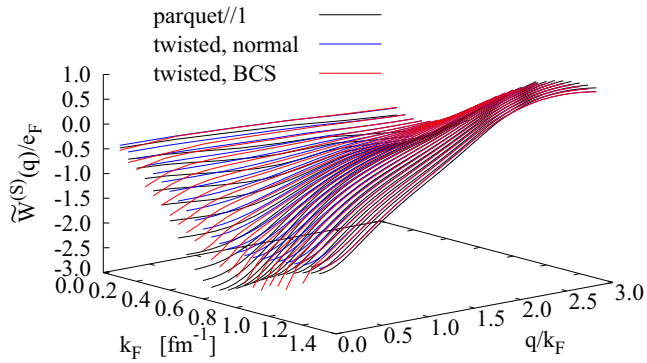

FIG. 7. The figure shows the density dependence of the singlet pairing interaction in both "parquet//1" approximation (black lines) and including both "beyond parquet" corrections and those stemming from using a superfluid Lindhard function (red lines).

of $-0.5e_F$, and that value of the Lindhard function changes by about 20%, can change the induced interaction by a factor of 2 which is seen in the left part of Fig. 4. This finding is consistent with the observation that the effect is smaller when nonparquet diagrams are included because the magnitude of $\tilde{V}_{\rm p-h}(0+)$ is decreased. Of course, it must be kept in mind that the agreement between the F_0^s obtained from $\tilde{V}_{\rm p-h}(0+)$, see Eq. (2.20), and that obtained from the hydrodynamic speed of sound, Eq. (3.3), is only approximate [16].

The similarly significant change of the longitudinal part of the effective interaction, as shown in the right part of Fig. 4, is much more expected and comparable in both parquet and "beyond parquet" results. As we go to higher density, see Figs. 5, the effects become smaller simply due to the fact that the superfluid gap becomes smaller, but they are still quite visible.

Since we are concerned with $^1S_0$ pairing, we need to map the $\mathbb{1}$, $\hat{L}$, and $\hat{T}$ channel interactions onto the S wave,

$$\widetilde{W}^{(S)}(q) = \widetilde{W}^{(\mathbb{1})}(q) - \widetilde{W}^{(L)}(q) - 2\widetilde{W}^{(T)}(q). \tag{3.4}$$

The interactions are shown in Fig. 6. Somewhat unexpectedly, the results show much less effect from using the superfluid Lindhard functions. The reason is found in the fact that the corrections go, in both the central and the spin channels, in the same direction and lead to an apparent partial cancellation, see Eq. (3.4). We could not see an argument that this cancellation is generic, but rather we consider it a coincidence.

Figure 7 gives an overall account of the density dependence of the S-wave pairing interaction. Generally, the inclusion of "beyond-parquet" diagrams reduces the interaction strength, the effect is most pronounced at intermediate densities. We also see clearly that the corrections from using a superfluid Lindhard function are smaller, with increasing density, at longer wavelengths which is due to the fact that the gap gets smaller.

C. BCS pairing

Once the ground-state correlations and effective interactions are known, the superfluid gap function $\Delta_{\mathbf{k}}$ can be determined by solving the gap equation (2.17).

The gap equation was solved by the eigenvalue method with an adaptive mesh as outlined in the Appendix of Ref. [15]. We have adopted a free single-particle spectrum for $e_{\mathbf{k}}$ as it occurs in Eqs. (2.14) and (2.17). One could also use the actual spectrum of CBF single-particle energies [39], in both the pairing interaction (2.14) and the denominator of Eq. (2.17). We have discussed and studied the effect of these modifications in previous work [32], there is no reason for repetition. A recent very extensive comparison with earlier work [35,41,54,59–65] is found in Ref. [36]. We can, therefore, focus in this paper on the aspect where we went beyond previous work [25,32].

Our results for the superfluid gap for the two potentials are shown in Fig. 8. Evidently the difference of the gap between these two potential models is almost negligible and certainly within the accuracy of both the FHNC/parquet//1 approximation. We have above shown that specific "beyond parquet"

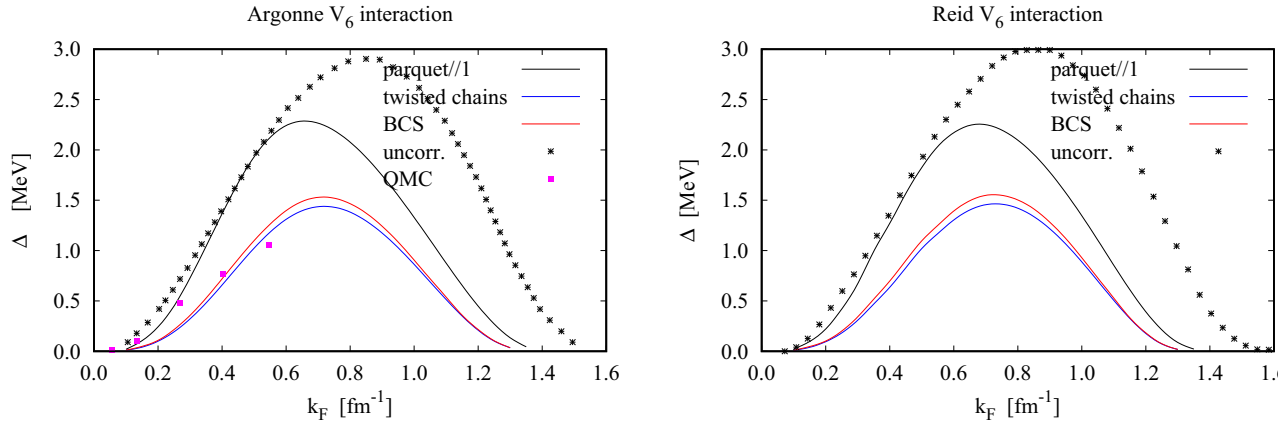

FIG. 8. Superfluid gap Δ_{k_F} at the Fermi momentum as a function of Fermi wave number k_F for the Argonne V_6 interaction (left figure) and the Reid V_6 potential (right figure). We show the parquet calculation (black curve), the "beyond parquet" results (blue curve) using the Lindhard function for normal systems, and the "beyond parquet" results using the superfluid Lindhard function (red curves). The crosses show the results for the bare Argonne and Reid interactions, these data are from Ref. [66]. The magenta squares in the left figure are quantum Monte Carlo data from Ref. [67].

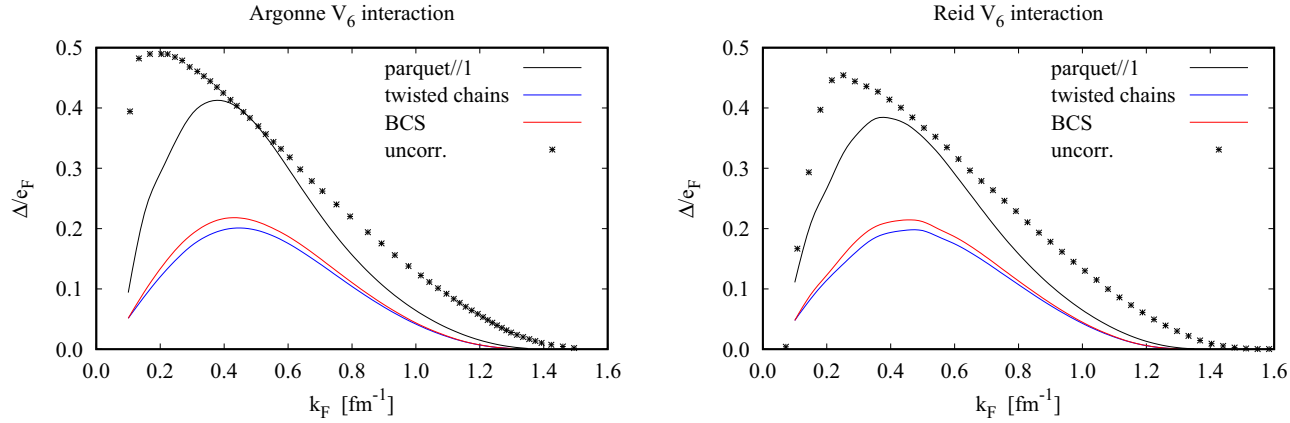

FIG. 9. Same as Fig. 8 for the gap in units of the Fermi energy of the noninteracting Femri gas.

corrections to the effective interaction should enhance the repulsion between particles in the singlet state, and Figs. 8 and 9 show exactly this effect. In fact, these contributions bring our results quite close to the quantum Monte Carlo data of Ref. [67]. On the other hand, the influence of using a superfluid Lindhard function appears modest. Considering that inspection of the individual pieces of the effective interactions suggests exactly the opposite, we conclude that our specific results are circumstantial and may well be totally different for other interactions or, for example, *P*-wave pairing.

In comparison to the quantum Monte Carlo data of Ref. [67] it must, of course, be noted that our interaction model is somewhat different. We have used the full v_6 interaction, wheras Ref. [67] uses the *S*-wave part of the Argonne potential. We have tried to use that interaction, too, but it turned out that the pure *S*-wave interaction leads to a spinodal instability in which case the parquet equations have no solution.

IV. SUMMARY AND PROSPECTS

The work reported in this paper represents the most rigorous calculation yet performed for nuclear systems within correlated BCS theory. We have described new calculations of the pairing gap in the $^1S_0$ partial-wave channel.

Our work goes beyond the calculations reported in Ref. [32] in several important aspects: We have replaced the state-independent FHNC/parquet summation method by the state-dependent parquet summation method [16]. We have also included the leading "beyond parquet" corrections [17], the reason for why these diagrams can be important in particular in the $^1S_0$ interaction channel has been discussed in the introduction in connection with Fig. 1. Finally, we have used a superfluid Lindhard function for the calculation of the particle-hole propagator. We found that each of these effects is quite substantial and the fact that the sum of all of these corrections is modest seems circumstantial rather than generic.

We need to reiterate the importance of the energy numerator term which originates from the fact that the correlated BCS theory is formulated in terms of what should be considered a static approximation of the T matrix. We have examined, in Eq. (2.43), the relationship between low-order variational calculations and the analysis of the gap equation due to Cooper, Mills, and Sessler (see also Ref. [68]). An important issue is the demonstration of how Jastrow-Feenberg correlations assume the task of short-ranged screening which is otherwise accomplished by the pair wave function $\chi(r)$, Eq. (2.42). This works, of course, only for state-dependent interactions if the correlations are optimized in each operator channel separately. This casts some doubts on earlier calculations of the superfluid gap, including our own [25,32], which use state-independent correlation functions.

Improvements can be sought in different ways: To look at *P*-wave pairing, we need to extend the theory to include a spin-orbit interaction. Another option is to add some phenomenological information into the particle-hole interaction $\hat{V}_{\mathrm{p-h}}(q)$ in order to enforce the agreement between the Fermi liquid parameter F_0^s obtained from the long-wavelength limit (2.20) and from the hydrodynamic derivative (3.3). To do the same for F_0^a requires to extend the theory to arbitrary spin polarization. Work along these lines is in progress.

Another important aspect that we have not touched in this paper is the importance of three-body interactions. There is the general consensus that three-body interactions are important in nuclear systems at higher densities. The literature on the issue is vast, see Ref. [69] for a recent discussion. For the problem at hand, three-body forces are expected to be most important for *P*-wave pairing at high densities, see, e.g., Ref. [70] and Ref. [71] for a very complete discussion of the earlier literature and, in particular, the sensitivity of the pairing gap on the choice of the interaction. A generalization of parquet theory for three-body forces could be carried out along the lines of three-body Jastrow-Feenberg [72,73] or parquet theory [74] but has not been carried out so far. We hesitate very much to speculate what the effect of including three-body forces in parquet/CBF theory would do, a solid calculation would go far beyond the scope of this paper.

ACKNOWLEDGMENTS

Encouragement for this work was derived from a workshop on *Nuclear Many-Body Theories: Beyond the Mean Field Approaches* at the Asia Pacific Center for Theoretical Physics in Pohang, South Korea, in July 2019 and the winter school

on *Superfluidity and Transport for Multimessenger Physics of Compact Stars* in Karpacz, Poland, February 2020.

APPENDIX: CORRELATED BASIS FUNCTIONS THEORY

For the development of a microscopic theory for superfluid systems we need the basic ingredients of CBF theory. We give here only the definitions of the relevant quantities to the extent that they are needed for the present work, details may be found in pedagogical material [9] and review articles [8,24].

CBF theory uses the correlation operator F to generate a complete set of correlated and normalized N-particle basis states through

$$\left|\Psi_{\mathbf{m}}^{(N)}\right\rangle = \frac{F_N\,|\mathbf{m}^{(N)}\rangle}{\langle\mathbf{m}^{(N)}|F_N^\dagger F_N\,|\mathbf{m}^{(N)}\rangle^{1/2}}, \tag{A1}$$

where the $\{|\mathbf{m}^{(N)}\rangle\}$ form a complete basis of model states, normally consisting of Slater determinants of single-particle orbitals.

In general, we label "hole" states which are occupied in $|\mathbf{o}\rangle$ by h, h', h_i , . . . , and unoccupied "particle" states by p, p', p_i, and so on. To display the particle-hole pairs explicitly, we will alternatively to the notation $|\mathbf{m}\rangle$ use $|\Psi_{p_1\ldots p_d\,h_1\ldots h_d}\rangle$. A basis state with d particle-hole pairs is then

$$|\Psi_{p_1\ldots p_d\,h_1\ldots h_d}\rangle = \left[I^{(N)}_{p_1,\ldots h_1}\right]^{-1/2} F_N a^\dagger_{p_1}\cdots a^\dagger_{p_d} a_{h_d}\cdots a_{h_1}|\mathbf{o}\rangle. \tag{A2}$$

For the off-diagonal elements $O_{\mathbf{m},\mathbf{n}}$ of an operator $\hat{O}$, we sort the quantum numbers m_i and n_i such that $|\mathbf{m}\rangle$ is mapped onto $|\mathbf{n}\rangle$ by

$$|\mathbf{m}\rangle = a^\dagger_{m_1} a^\dagger_{m_2}\cdots a^\dagger_{m_d}\, a_{n_d}\cdots a_{n_2} a_{n_1}|\mathbf{n}\rangle. \tag{A3}$$

From this we recognize that, to leading order in the particle number N, any matrix element of an operator $\hat{O}$

$$O_{\mathbf{m},\mathbf{n}} = \langle\Psi_{\mathbf{m}}|\hat{O}|\Psi_{\mathbf{n}}\rangle \tag{A4}$$

depends only on the *difference* between the states $|\mathbf{m}\rangle$ and $|\mathbf{n}\rangle$, and *not* on the states as a whole. Consequently, $O_{\mathbf{m},\mathbf{n}}$ can be written as matrix element of a d-body operator

$$O_{\mathbf{m},\mathbf{n}} \equiv \langle m_1\, m_2\, \ldots m_d\,|\mathcal{O}(1,2,\ldots d)\,|n_1\, n_2\, \ldots n_d\rangle_a. \tag{A5}$$

(The index a indicates antisymmetrization.)

The key quantities for the execution of the theory are diagonal and off-diagonal matrix elements of unity and $H-H_{\mathbf{o}}$,

$$M_{\mathbf{m},\mathbf{n}} = \langle\Psi_{\mathbf{m}}|\Psi_{\mathbf{n}}\rangle \equiv \delta_{\mathbf{m},\mathbf{n}} + N_{\mathbf{m},\mathbf{n}}, \tag{A6}$$

$$W_{\mathbf{m},\mathbf{n}} = \langle\Psi_{\mathbf{m}}|H - \tfrac{1}{2}(H_{\mathbf{m}} + H_{\mathbf{n}})|\Psi_{\mathbf{m}}\rangle. \tag{A7}$$

Equation (A7) defines a natural decomposition [9,39] of the matrix elements of H into the off-diagonal quantities $W_{\mathbf{m},\mathbf{n}}$ and $N_{\mathbf{m},\mathbf{n}}$ and diagonal quantities $H_{\mathbf{m}}$.

To leading order in the particle number, the *diagonal* matrix elements of $H-H_{\mathbf{o}}$ become additive, so that for the above d-pair state we can define the CBF single particle energies

$$\langle\Psi_{\mathbf{m}}|H-H_{\mathbf{o}}|\Psi_{\mathbf{m}}\rangle \;\equiv\; \sum_{i=1}^{d} e_{p_i h_i} + \mathcal{O}(N^{-1}), \tag{A8}$$

with $e_{\rm ph} = e_p - e_h$, where

$$\begin{aligned} e_p &= \;\langle\Psi_p|\; H-H_{\mathbf{o}}|\Psi_p\rangle = t(p) + u(p), \\ e_h &= -\langle\Psi_h|\,H-H_{\mathbf{o}}|\Psi_h\rangle \;= t(h) + u(h), \end{aligned} \tag{A9}$$

and $u(p)$ is an average field that can be expressed in terms of the compound diagrammatic quantities of FHNC theory [39].

According to (A5), $W_{\mathbf{m},\mathbf{n}}$ and $N_{\mathbf{m},\mathbf{n}}$ define d-particle operators $\mathcal{N}$ and $\mathcal{W}$, e.g.,

$$\begin{aligned} N_{\mathbf{m},\mathbf{o}} &\equiv N_{p_1 p_2\ldots p_d\,h_1 h_2\ldots h_d,0} \\ &\equiv \langle p_1 p_2\ldots p_d\,|\,\mathcal{N}(1,2,\ldots,d)\,|\,h_1 h_2\ldots h_d\rangle_a, \\ W_{\mathbf{m},\mathbf{o}} &\equiv W_{p_1 p_2\ldots p_d\,h_1 h_2\ldots h_d,0} \\ &\equiv \langle p_1 p_2\ldots p_d\,|\,\mathcal{W}(1,2,\ldots,d)\,|\,h_1 h_2\ldots h_d\rangle_a. \end{aligned} \tag{A10}$$

Diagrammatic representations of $\mathcal{N}(1,2,\ldots,d)$ and $\mathcal{W}(1,2,\ldots,d)$ have the same topology [39]. In homogeneous systems, the continuous parts of the p_i, h_i are wave numbers $\mathbf{p}_i$, $\mathbf{h}_i$; we abbreviate their difference as $\mathbf{q}_i$.

In principle, the $\mathcal{N}(1,2,\ldots,d)$ and $\mathcal{W}(1,2,\ldots,d)$ are nonlocal d-body operators. Above, we have shown that we need, for examining pairing phenomena, only the two-body operators. Moreover, the low density of the systems we are examining permits the same simplifications of the FHNC theory that we have spelled out in Sec. II A. In that approximation, the operators $\mathcal{N}(1,2)$ and $\mathcal{W}(1,2)$ are local, and we have [24]

$$\begin{aligned} &\mathcal{N}(1,2) = \mathcal{N}(r_{12}) = \Gamma_{\rm dd}(r_{12}) \\ &\mathcal{W}(1,2) = \mathcal{W}(r_{12}), \quad \tilde{\mathcal{W}}(k) \equiv \tilde{W}(k) = -\frac{t(k)}{S_F(k)}\tilde{\Gamma}_{\rm dd}(k). \end{aligned} \tag{A11}$$

[1] R. Broglia and V. Zelevensky, *Fifty Years of Nuclear BCS* (World Scientific, Singapore, 2013).

[2] A. Bohr, B. R. Mottelson, and D. Pines, Phys. Rev. **110**, 936 (1958).

[3] J. Bardeen, L. N. Cooper, and J. R. Schrieffer, Phys. Rev. **108**, 1175 (1957).

[4] L. N. Cooper, R. L. Mills, and A. M. Sessler, Phys. Rev. **114**, 1377 (1959).

[5] J. W. Clark and C.-H. Yang, Lett. Nuovo Cimento **3**, 272 (1970).

[6] C.-H. Yang and J. W. Clark, Nucl. Phys. A **174**, 49 (1971).

[7] C.-H. Yang, Ph.D. thesis, Washington University, 1971.

[8] J. W. Clark, in *Progress in Particle and Nuclear Physics*, Vol. 2, edited by D. H. Wilkinson (Pergamon Press Ltd., Oxford, 1979), pp. 89–199.

[9] E. Krotscheck, in *Introduction to Modern Methods of Quantum Many–Body Theory and Their Applications*, Advances in

Quantum Many–Body Theory, Vol. 7, edited by A. Fabrocini, S. Fantoni, and E. Krotscheck (World Scientific, Singapore, 2002), pp. 267–330.
[10] H. K. Sim, C.-W. Woo, and J. R. Buchler, Phys. Rev. A **2**, 2024 (1970).
[11] A. D. Jackson, A. Lande, and R. A. Smith, Phys. Rep. **86**, 55 (1982).
[12] A. D. Jackson, A. Lande, and R. A. Smith, Phys. Rev. Lett. **54**, 1469 (1985).
[13] E. Krotscheck, R. A. Smith, and A. D. Jackson, Phys. Rev. B **24**, 6404 (1981).
[14] E. Krotscheck and J. W. Clark, Nucl. Phys. A **333**, 77 (1980).
[15] H.-H. Fan, E. Krotscheck, T. Lichtenegger, D. Mateo, and R. E. Zillich, Phys. Rev. A **92**, 023640 (2015).
[16] E. Krotscheck and J. Wang, Phys. Rev. C **101**, 065804 (2020).
[17] E. Krotscheck and J. Wang, Phys. Rev. C **102**, 064305 (2020).
[18] R. V. Reid, Jr., Ann. Phys. (NY) **50**, 411 (1968).
[19] H. A. Bethe and M. B. Johnson, Nucl. Phys. A **230**, 1 (1974).
[20] B. D. Day, Phys. Rev. C **24**, 1203 (1981).
[21] R. B. Wiringa, V. G. J. Stoks, and R. Schiavilla, Phys. Rev. C **51**, 38 (1995).
[22] R. B. Wiringa, R. A. Smith, and T. L. Ainsworth, Phys. Rev. C **29**, 1207 (1984).
[23] E. Feenberg, *Theory of Quantum Fluids* (Academic, New York, 1969).
[24] E. Krotscheck, J. Low Temp. Phys. **119**, 103 (2000).
[25] H.-H. Fan and E. Krotscheck, Phys. Rep. **823**, 1 (2019).
[26] V. R. Pandharipande and R. B. Wiringa, Nucl. Phys. A **266**, 269 (1976).
[27] S. Fantoni and S. Rosati, Nuovo Cimento A **43**, 413 (1978).
[28] V. R. Pandharipande and R. B. Wiringa, Rev. Mod. Phys. **51**, 821 (1979).
[29] E. Krotscheck, Phys. Rev. A **26**, 3536 (1982).
[30] E. Krotscheck, Nucl. Phys. A **482**, 617 (1988).
[31] R. A. Smith and A. D. Jackson, Nucl. Phys. A **476**, 448 (1988).
[32] H.-H. Fan, E. Krotscheck, and J. W. Clark, J. Low Temp. Phys. **189**, 470 (2017).
[33] A. D. Jackson, E. Krotscheck, D. Meltzer, and R. A. Smith, Nucl. Phys. A **386**, 125 (1982).
[34] J. M. C. Chen, J. W. Clark, E. Krotscheck, and R. A. Smith, Nucl. Phys. A **451**, 509 (1986).
[35] A. Fabrocini, S. Fantoni, A. Y. Illarionov, and K. E. Schmidt, Phys. Rev. Lett. **95**, 192501 (2005).
[36] G. E. Pavlou, E. Mavrommatis, C. Moustakidis, and J. W. Clark, Eur. Phys. J. A **53**, 96 (2017).
[37] O. Benhar, G. D. Rosi, and G. Salvi, J. Low Temp. Phys. **189**, 250 (2017).
[38] A. J. Leggett, $p+ip$ Fermi superfluids: Old results and new questions,, Invited Talk, presented at the 2018 International Symposium on Quantum Fluids and Solids, Tokyo (2018).
[39] E. Krotscheck and J. W. Clark, Nucl. Phys. A **328**, 73 (1979).
[40] A. L. Fetter and J. D. Walecka, *Quantum Theory of Many-Particle Systems* (McGraw–Hill, New York, 1971).
[41] S. Gandolfi, A. Y. Illarionov, F. Pederiva, K. E. Schmidt, and S. Fantoni, Phys. Rev. C **80**, 045802 (2009).
[42] A. D. Jackson and R. A. Smith, Phys. Rev. A **36**, 2517 (1987).
[43] J. Lindhard, K. Dan. Vidensk. Selk. Mat.-Fys. Med. **28**, 1 (1954).
[44] K.-K. Voo, W. C. Wu, J.-X. Li, and T. K. Lee, Phys. Rev. B **61**, 9095 (2000).
[45] R. Combescot, M. Y. Kagan, and S. Stringari, Phys. Rev. A **74**, 042717 (2006).
[46] A. W. Steiner and S. Reddy, Phys. Rev. C **79**, 015802 (2009).
[47] E. Vitali, H. Shi, M. Qin, and S. Zhang, J. Low Temp. Phys. **189**, 312 (2017).
[48] J. R. Schrieffer, *Theory of Superconductivity (Advanced Books Classics)*, revised ed. (Perseus Books, New York, 1999).
[49] H.-Y. Kee and C. M. Varma, Phys. Rev. B **58**, 15035 (1998).
[50] H.-Y. Kee and Y. B. Kim, Phys. Rev. B **59**, 4470 (1999).
[51] H.-J. Schulze, A. Polls, and A. Ramos, Phys. Rev. C **63**, 044310 (2001).
[52] C. J. Pethick and H. Smith, *Bose-Einstein Condensation in Dilute Gases*, 2nd ed. (Cambridge University Press, Cambridge, UK, 2008).
[53] R. Jastrow, Phys. Rev. **98**, 1479 (1955).
[54] A. Fabrocini, S. Fantoni, A. Y. Illarionov, and K. E. Schmidt, Nucl. Phys. A **803**, 137 (2008).
[55] S. Babu and G. E. Brown, Ann. Phys. (NY) **78**, 1 (1973).
[56] W. Guo, U. Lombardo, and P. Schuck, Phys. Rev. C **99**, 014310 (2019).
[57] S. Shlomo, V. M. Kolomietz, and G. Colò, Eur. Phys. J. A **30**, 23 (2006).
[58] E. Krotscheck and J. Wang, Phys. Lett. B **809**, 135770 (2020).
[59] J. Wambach, T. Ainsworth, and D. Pines, Nucl. Phys. A **555**, 128 (1993).
[60] H.-J. Schulze, J. Cugnon, A. Lejeune, M. Baldo, and U. Lombardo, Phys. Lett. B **375**, 1 (1996).
[61] A. Schwenk, B. Friman, and G. E. Brown, Nucl. Phys. A, **713** 191 (2003).
[62] H. Müther and W. H. Dickhoff, Phys. Rev. C **72**, 054313 (2005).
[63] L. G. Cao, U. Lombardo, and P. Schuck, Phys. Rev. C **74**, 064301 (2006).
[64] S. Yoshida and H. Sagawa, Phys. Rev. C **77**, 054308 (2008).
[65] D. Ding, A. Rios, H. Dussan, W. H. Dickhoff, S. J. Witte, A. Carbone, and A. Polls, Phys. Rev. C **94**, 025802 (2016).
[66] V. A. Khodel, V. V. Khodel, and J. W. Clark, Nucl. Phys. A **598**, 390 (1996).
[67] A. Gezerlis and J. Carlson, Phys. Rev. C **77**, 032801(R) (2008).
[68] P. Noziéres and S. Schmitt-Rink, J. Low Temp. Phys. **59**, 195 (1985).
[69] L. Coraggio, J. W. Holt, N. Itaco, R. Machleidt, L. E. Marcucci, and F. Sammarruca, Phys. Rev. C **89**, 044321 (2014).
[70] W. Zuo, C. X. Cui, U. Lombardo, and H.-J. Schulze, Phys. Rev. C **78**, 015805 (2008).
[71] P. Papakonstantinou and J. W. Clark, J. Low Temp. Phys. **189**, 361 (2017).
[72] C. W. Woo, Phys. Rev. Lett. **28**, 1442 (1972).
[73] C. W. Woo, Phys. Rev. A **6**, 2312 (1972).
[74] A. D. Jackson, A. Lande, R. W. Guitink, and R. A. Smith, Phys. Rev. B **31**, 403 (1985).